Biochimica et Biophysica Acta, 982 (1989) 196–204
Elsevier

BBAMEM 74474

Reorientational dynamics in lipid vesicles and liposomes studied with ESR: effects of hydration, curvature and unsaturation

Leo J. Korstanje, Ernst E. van Faassen and Yehudi K. Levine

Department of Molecular Biophysics, Buys Ballot Laboratory, Rijksuniversiteit Utrecht, Utrecht (The Netherlands)

(Received 15 February 1989)

Key words: Phospholipid; Curvature; Reorientational dynamics; ESR; Cholestane spin label; Lipid vesicle; Hydration

Electron spin resonance experiments were carried out on 3-doxyl-5α-cholestane spin-label (CSL) molecules embedded in multilamellar liposomes and small unilamellar vesicles (SUVs) of palmitoyloleoylphosphatidylcholine (POPC), dioleoylphosphatidylcholine (DOPC) and dilinoleoylphosphatidylcholine (DLPC). The experimental spectra were analyzed by a numerical solution of the stochastic Liouville equation. Effects of temperature, presence of unsaturated bonds and high bilayer curvature on the dynamic behaviour of the lipid molecules were studied. Our results, combined with results from planar multibilayers with a varying hydration rate (Korstanje et al. (1989) Biochim. Biophys. Acta 980, 225–233), give a consistent picture of the orientational order and rotational dynamics of CSL molecules embedded in lipid matrices with various geometrical configurations. Increase of hydration or temperature reduces molecular ordering and increases molecular dynamics. In highly curved vesicle configurations, SUVs, molecular order is found to be lower than in multilamellar liposomes. In contrast, rotational motion is not affected by increase of curvature. In all lipid configurations studied, increase of the number of unsaturated bonds in the fatty acid chains reduces molecular ordering. We find, however, no effect of unsaturation on the rotational mobility of the CSL probe molecules. These results clearly show that changes in molecular orientational order and reorientational dynamics have to be considered separately, and that they are not necessarily correlated as implied by the common concept of membrane fluidity. Comparing our results with data from a motional narrowing analysis shows that the latter approach seriously overestimates the rate of molecular reorientation.

Introduction

Knowledge of the dynamic behaviour of lipid molecules is of great importance for a proper insight in the functional properties of biological membranes. This behaviour is often studied in model systems consisting of supramolecular assemblies of lipid molecules. The motion of the lipid molecules in these systems is characterized by a strong anisotropy so that a description of their physical properties must incorporate not only dynamic processes, but also orientational order on a microscopic scale. These properties of model systems depend not only on intrinsic parameters such as chemical composition, temperature and hydration. They are also determined by the geometrical packing configuration of the molecules associated with the structure of the assembly; planar bilayers, hexagonal structures, SUVs or multilamellar liposomes. These liposomes are simply unsonicated aqueous dispersions of the lipid molecules. Henceforth, we shall use the term liposome to denote an aqueous dispersion of lipid molecules.

The important question now arises as to whether the experimental observation on the different configurations yield a consistent picture of molecular behaviour, once the configurational differences are taken into account. Although the question about consistency has been posed in earlier studies [1–3], no clear answer has yet emerged. A ^{2}H-NMR study [2] has shown that the internal molecular motion and order of lipid chains packed in SUVs are very similar to those in liposomes. The only significant differences were found for C-D bonds near the terminal methyl groups of the chains, where the order parameters in the SUV's were 10–30% smaller than those for liposomes. However, the interpretation of the relaxation times in terms of detailed chain dynamics is not a trivial task. Time-resolved fluorescence anisotropy studies on 1,6-diphenyl-1,3,5-hexatriene (DPH) molecules embedded in SUVs and liposomes of dipalmitoylphosphatidylcholine (DPPC)

Correspondence: L.J. Korstanje, Department of Molecular Biophysics, Buys Ballot Laboratory, Rijksuniversiteit Utrecht, Princetonplein 5, 3584 CC Utrecht, The Netherlands.

have indicated a lower degree of ordering for the probe molecules embedded in SUVs [3]. An ESR study of fatty acid spin-labels in egg PC and DPPC liposomes has indicated a higher degree of order than that found in planar multibilayers of the same lipids [1]. The interpretation of this work has been questioned [4,5], particularly as it may be compromised by conformational changes in the fatty acid chains resulting from the attachment of the bulky nitroxide group. Moreover, as the applicability of spectral analysis based on the motional narrowing approximation has not been validated, the conclusions about the order parameters and the rotational correlation times may be incorrect [6]. The latter ambiguities in the interpretation of the ESR experiments, however, can be avoided in an approach which takes into account slow molecular motions [7–10]. We shall in fact show that the widely used motional-narrowing approximation is not valid for the lipid systems studied here and its application seriously overestimates the rates of molecular reorientational motions.

We shall here address part of the consistency question posed above and compare the results from ESR experiments on the cholestane spin-label (CSL) molecules embedded in SUV, liposome and planar bilayer configurations of phospholipids of different fatty acid composition. These systems differ not only in their macroscopic geometry, but also in the hydration rate of the lipid headgroups. Previous work in our laboratory on planar multibilayers [11–13] has shown that the hydration of the headgroups affects both the molecular ordering and rotational dynamics. We thus expect these experimental results to differ from those obtained from SUV and liposome configurations, where the headgroups are completely hydrated. On the other hand, a comparison of the results from the two latter configurations yields insight into the effects of the radius of curvature of the bilayer structure.

Materials and Methods

Palmitoyloleoylphosphatidylcholine (POPC) and dioleoylphosphatidylcholine (DOPC) were purchased from Sigma Chemical Co. (St. Louis, MO, USA). Dilinoleoylphosphatidylcholine (DLPC) was obtained from Lipid Products (Surrey, UK). The spin label 4′,4′-dimethylspiro[5α-cholestane-3,2′-oxazolidin]-3′-yloxy (CSL) was bought from Aldrich Chemical Co. (Milwaukee, WI, U.S.A.). When necessary, the purity of the lipids and the spin label was checked by high performance thin layer chromatography (HPTLC).

In all our experiments, a CSL concentration of 1 mol% was used. At this concentration, the spin–spin interactions between individual CSL molecules are expected to produce homogeneous line broadening of approx. 0.5 G [14]. This value is comfortably exceeded by the combined effect of Lorentzian and Gaussian broadening of approx. 1.5 G.

Sample preparation

The lipid/CSL mixtures were prepared by dissolving the components in chloroform. After mixing, the chloroform was removed by a flow of nitrogen gas and subsequent storage under vacuum for several hours. The lipid/CSL mixture was hydrated by the addition of a 20 mM Tris buffer (pH 8.0), containing 7.5 μM EDTA. The resulting mixture, containing 2 mg lipid/ml buffer, was homogenized with a vortex mixer for several minutes.

Liposome samples contained 20 μl of the hydrated lipid/CSL mixture in a quartz capillary. SUV's were obtained by sonication of the vortexed lipid/CSL mixture in a bath type sonicator for 15–45 minutes. The clear suspension was subsequently centrifuged at 40000 $\times g$ for 60 min at 4°C. 20 μl of the supernatant, containing 2 mg lipid/ml, was put in a quartz capillary and was used as a sample.

All the preparative steps were carried out in the dark under a nitrogen atmosphere as much as possible to avoid oxidation of the lipids. The samples were used in the ESR experiments within 24 h of their preparation.

ESR experiments

ESR experiments were carried out using a Varian E-9 X-band spectrometer, equipped with a TM110 cavity. The sample temperature was regulated within 1 C° with a Varian V4540 variable temperature accessory and measured by a copper-constantan thermocouple placed above the sample, just outside the active region of the cavity. ESR spectra were recorded at a microwave power level of 10–15 mW, well below saturation. A magnetic field modulation of 1.0–1.6 Gauss top-top with a frequency of 100 kHz was used to detect the first derivative of the absorption signal. The background ESR signal, arising from the quartz capillary, was subtracted from the measurements before analysis.

Spectral simulations

The simulation of the experimental ESR spectra was carried out by a numerical solution of the stochastic Liouville equation (SLE) for the density matrix of a spin-label molecule. This approach provides spectral simulations for a wide range of rotational correlation times of the CSL molecules, from very slow motions ($\tau \approx 10^{-6}$ s) to very fast motions ($\tau \ll 10^{-9}$ s) of the CSL molecules in the liquid-crystalline phase. The technical details of the analysis are described elsewhere [7–9,15–17] and the method will only be summarized below.

The SLE is the equation of motion for the density matrix of a collection of non-interaction spin-label molecules. The effect of the surrounding ordered lipid matrix on the spin-labels enters the SLE in the form of a relaxation term determined by an anisotropic diffusion operator. The solutions of the SLE allow the computation of the magnetization of and power absorption by the spin labels.

In our case the relaxation term involves the standard rotational diffusion model [18,19], where the molecules are assumed to undergo small-step, correlated, angular excursions subject to the action of an orienting potential $U(\Omega)$ [20]. This potential is taken to be cylindrically symmetric around the normal to the bilayer surface:

$$U(\Omega) = U(\beta) = -kT\{\lambda_2 P_2(\cos\beta) + \lambda_4 P_4(\cos\beta)\} \tag{1}$$

where β is the angle between the long axis of the spin probe and the local director to the bilayer surface. P_2 and P_4 denote Legendre polynomials of order 2 and 4:

$$P_2(\cos\beta) = 1/2(3\cos^2\beta - 1) \tag{2}$$

$$P_4(\cos\beta) = 1/8(35\cos^4\beta - 30\cos^2\beta + 3) \tag{3}$$

In view of the geometrical form of the CSL molecule, its rotational diffusion in the membrane is assumed to be cylindrically symmetric, with a rotational diffusion tensor of the form $\bar{\bar{D}} = \mathrm{diag}\,(D_\perp, D_\perp, D_\parallel)$, where $D_\parallel$ and $D_\perp$ are the diffusion rates for rotations around the long molecular axis and rotation of that axis, respectively. The orientational distribution function $f(\beta)$ is given by:

$$f(\beta) = \frac{\exp(-U(\beta)/kT)}{\int_0^\pi \exp(-U(\beta)/kT)\sin\beta\,\mathrm{d}\beta} \tag{4}$$

The orientational order parameter $\langle P_2 \rangle$ is given by the average of the second order Legendre polynomial:

$$\langle P_2 \rangle = \int_{-1}^{1} f(\beta) P_2(\cos\beta)\,\mathrm{d}\cos\beta \tag{5}$$

$\langle P_4 \rangle$ is defined analogously:

$$\langle P_4 \rangle = \int_{-1}^{1} f(\beta) P_4(\cos\beta)\,\mathrm{d}\cos\beta \tag{6}$$

In SUV and liposome suspensions, the directors to the lipid bilayers have a random distribution of orientations relative to the static magnetic field $\bar{H}_0$. On a macroscopic scale, the samples exhibit complete orientational disorder. In this case, the observed ESR signal $P(\omega)$ can be considered to be a superposition of spectra of randomly distributed planar bilayer samples:

$$P(\omega) = \mathrm{Im}\; Z(\omega) \tag{7a}$$

$$Z(\omega) = 1/2\int_0^\pi Z(\omega, \theta)\sin\theta\,\mathrm{d}\theta \tag{7b}$$

where $Z(\omega, \theta)$ is the response function of a planar bila[illegible]mple oriented at an angle θ relative to $\bar{H}_0$.

[illegible]quencies near resonance, where $Z(\omega, \theta)$ is a strongly peaked function of θ, a straightforward numerical evaluation of Eqn. 7 requires a very fine integration mesh demanding inordinate amounts of cpu time. We have therefore evaluated the integral using a subtraction method which presupposes knowledge of $Z(\omega, \theta)$ at only a small number of orientations θ. Details of the procedure are given in Appendix 1.

Additional line broadening is introduced into the spectrum by a Lorentzian broadening, denoted by a relaxation time T_2, and a Gaussian broadening, σ_G.

Results and Discussion

ESR experiments on CSL molecules embedded in macroscopically unoriented lipid bilayer systems, that is small unilamellar vesicles and multilamellar liposomes, have been carried out. The effects on the molecular order and dynamics caused by the introduction of unsaturation into the lipid chains were studied by comparing the spectra from POPC, DOPC and DLPC. ESR spectra were recorded at temperatures between 20 and 55 °C, well above the gel/liquid-crystalline phase transition.

CSL is anchored with the nitroxide group at the lipid/water interface. As this group is fixed to the rigid steroid nucleus [21], the experimental ESR spectra yield information about the overall orientation and rigid body motion of the probe molecules. In the liquid-crystalline phase, the average orientation of the long axis of the molecule is perpendicular to the bilayer plane [22–24].

The principal axes of the magnetic $\bar{\bar{g}}$- and $\bar{\bar{A}}$-tensors are assumed to coincide and have a diagonal form in the CSL reference frame. The right-handed reference frame is defined with the x-axis oriented along the N-O bond, the y-axis oriented along the $2p-\pi$ orbital of the nitrogen and the z-axis oriented along the long molecular axis. Good fits were obtained with the same values for the $\bar{\bar{g}}$- and $\bar{\bar{A}}$-tensor as used in the simulation of ESR spectra from planar multibilayer samples [11]:

$$\bar{\bar{g}} = \mathrm{diag}\,(2.0081, 2.0024, 2.0061)$$

$$\bar{\bar{A}} = \mathrm{diag}\,(5.6, 34.0, 5.3)$$

These values were kept constant throughout the simulations. The isotropic spin-spin relaxation time T_2 was fixed at $T_2 = 2 \cdot 10^{-7}$ s, resulting in a Lorentzian line broadening of 0.28 G.

The simulated lineshapes for the SUV and liposome configurations did not exhibit marked changes on varying the motional anisotropy $N \equiv D_\parallel / D_\perp$ and the pair of potential parameters λ_2 and λ_4, Eqn. 1, which unambiguously defines the order parameters $\langle P_2 \rangle$ and $\langle P_4 \rangle$.

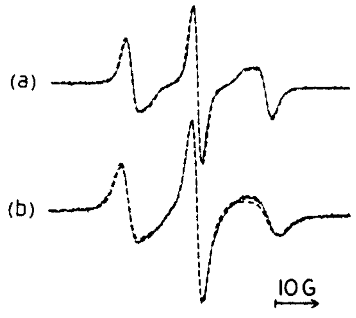

Fig. 1. Experimental (———) and simulated (— — —) ESR spectra of CSL in DOPC liposomes at (a) 55 °C and (b) 25 °C. The fitting parameters are:
(a) $D_\perp = 2.0 \cdot 10^8$ rad$^2 \cdot$s^{-1}, $\lambda_2 = 1.5$ and $\sigma_G = 1.2$ G
(b) $D_\perp = 5.0 \cdot 10^7$ rad$^2 \cdot$s^{-1}, $\lambda_2 = 2.0$ and $\sigma_G = 1.2$ G
Furthermore $D_\parallel = 5 D_\perp$ and $\lambda_4 = 0.4\ \lambda_2$.

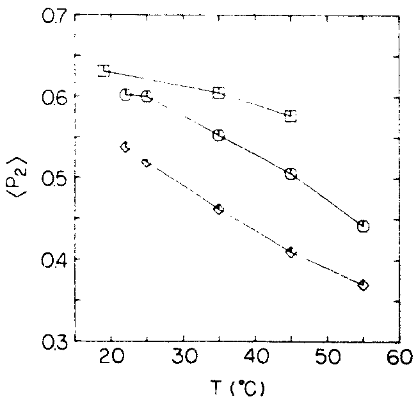

Fig. 2. Temperature dependence of the order parameter $\langle P_2 \rangle$ of CSL molecules embedded in SUVs and liposomes of POPC. Also included are the data obtained from CSL in planar lipid multibilayers with 24 wt.% water, Ref. 11. □, planar; ○, liposomes; ◇, SUVs.

This in contrast to the significant changes observed in simulations of spectra from planar multibilayers. This reduction in sensitivity is a reflection of the average over all the possible orientations of the local bilayer normal, which washes out the spectral details [25]. Nevertheless, the quality of the fit deteriorated gradually on increasing N beyond 10. We have therefore fixed this parameter rather arbitrarily to $N = 5$ close to the value of 4.7 expected from the geometry of the CSL molecule [26]. Furthermore, we were unable to obtain good fits on setting λ_4 equal to or close to zero as expected from our previous findings in planar multibilayer configurations [11]. This indicates that the CSL molecules have a broader orientation distribution function in SUV and liposome configurations than in the planar multibilayers. At the other extreme with $\lambda_4 \approx \lambda_2$, the simulations also yielded unsatisfactory fits. However, as this potential function corresponds to a bimodal distribution with maxima at $\beta = 0°$ and $\beta = 90°$, it is not expected to apply to the CSL molecules. In view of the foregoing we have fixed $\lambda_4 = 0.4\ \lambda_2$, thus providing the broadest possible distribution function exhibiting a monotonous decrease between $\beta = 0°$ and $\beta = 90°$.

These choices leave us with three adjustable fitting parameters; the rotational diffusion coefficient $D_\perp$, the potential parameter λ_2 and the Gaussian broadening σ_G. These fitting parameters are essentially not correlated. Thus the changes in the lineshape caused by varying one of them could not be compensated by changing the values of the other two parameters. We estimate the fitting parameters to be reliable within the following bounds: $D_\perp$, 30%; λ_2, 5% and σ_G, 10%. We found σ_G to be 1.2 G for all the SUV and liposome configurations, close to the values of approx. 1.1 G found in planar configurations [11].

The experimental and simulated spectra of CSL embedded in DOPC liposomes at two different tempera-

TABLE I

Best fit parameters for CSL in various lipid systems at $T = 35\,°C$

The lipid concentration in SUV and liposome suspensions was 2 mg/ml. The data for planar systems were taken from Ref. 11. The hydration rate of these systems was 24 wt.%. For SUVs and liposomes the estimated uncertainties are: $D_\perp$: 30%, λ_2: 5% and σ_G: 10%. Furthermore, $D_\parallel = 5D_\perp$ and $\lambda_4 = 0.4\ \lambda_2$ for these systems. $\langle P_2 \rangle$ and $\langle P_4 \rangle$ were calculated from λ_2 and λ_4 using Eqns. 5 and 6.

Lipid	System	σ_G (Gauss)	λ_2	λ_4	$D_\perp$ (10^8 rad$^2 \cdot$s^{-1})	$D_\parallel$ (10^8 rad$^2 \cdot$s^{-1})	$\langle P_2 \rangle$	$\langle P_4 \rangle$
POPC	planar	1.2	3.0	0.0	0.45	2.5	0.61	0.25
	liposomes	1.2	2.1	0.84	0.80	4.0	0.55	0.29
	vesicles	1.2	1.7	0.68	0.80	4.0	0.46	0.22
DOPC	planar	1.0	2.3	0.10	0.40	3.0	0.51	0.18
	liposomes	1.2	1.9	0.76	1.0	5.0	0.50	0.25
	vesicles	1.2	1.6	0.64	0.80	4.0	0.44	0.21
DLPC	planar	0.9	1.8	0.40	0.28	2.4	0.45	0.18
	liposomes	1.2	1.5	0.60	1.0	5.0	0.40	0.18
	vesicles	1.2	1.4	0.56	1.0	5.0	0.35	0.15

tures are shown in Fig. 1 to illustrate the temperature dependence of the spectra and the quality of the fits. The quality of a fit was judged visually and the procedure has been described by us in detail elsewhere [27].

Orientational order

The temperature dependence of the order parameter $\langle P_2 \rangle$ of CSL molecules embedded in POPC liposomes and SUVs is shown in Fig. 2. A clear decrease of $\langle P_2 \rangle$ with increasing temperature is found both in SUV and liposome configurations. Interestingly, the order parameters of CSL are lower in SUVs than in liposomes at every temperature within the range studied here. As the hydration rate of the lipid headgroups is identical in both configurations, we can conclude that high curvature of the bilayer reduces the degree of ordering of the CSL molecules in SUVs. This is corroborated by the findings with DOPC and DLPC (Table I). Our results thus conflict with the hypothesis that a small radius of curvature would result in a tighter molecular packing [28].

While a difference in the degree of ordering between SUV and liposome dispersions found here has been noted before in fluorescent anisotropy [3,29] and ^{2}H-NMR [30] experiments, it was not possible to trace the observed effect unambiguously to the difference in curvature. The results presented here clearly show that a high radius of curvature results in a lower ordering of the CSL molecules.

We note further that the order parameter $\langle P_2 \rangle$ of CSL is higher in planar lipid multibilayers containing 24 wt.% water than in dispersions of the same lipid (Table I and Fig. 2). This confirms the observations on planar multibilayers, that an increase of the hydration rate induces a decrease in the degree of molecular ordering [11,12,31]. It is interesting to note that the hydration dependence of $\langle P_2 \rangle$ in multibilayers [11] yields good agreement with $\langle P_2 \rangle$ for liposomes when extrapolated to 35 wt.% water content, characteristic of the maximum hydration of liposomes and SUVs [32].

Turning to the effects of unsaturation in SUVs and liposomes, we find that $\langle P_2 \rangle$ decreases significantly on increasing the number of unsaturated bonds in the fatty acid chains (Table I). This is in agreement with previous studies of curved and planar configurations [11,13,33–35].

Reorientational dynamics

The temperature dependence of the rotational diffusion constant $D_\perp$ of CSL in POPC bilayer configurations is shown in Fig. 3. As with the order parameters above, we find a clear temperature dependence with $D_\perp$ increasing by a factor of around 5 over the temperature range 20–55°C. In contrast with the behaviour of the order parameters, the diffusion constants coincide within the accuracy of the fits for SUVs and liposomes (Table I). We thus conclude that the rotational mobility of CSL molecules embedded in these bilayer configurations is not affected by the radius of curvature.

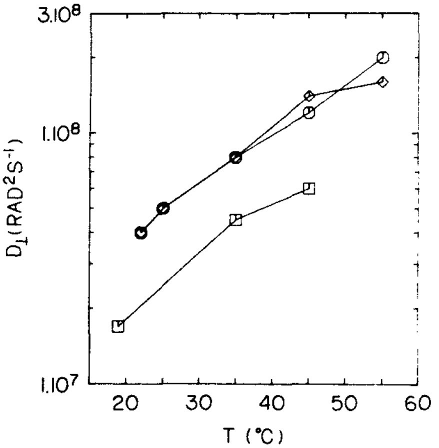

Fig. 3. Temperature dependence of the rotational diffusion parameter $D_\perp$ of CSL molecules embedded in various lipid systems of POPC. The data for planar lipid multibilayers, containing 24 wt.% water, were taken from Ref. 11. □, planar; ○, liposomes; ◇, SUVs.

It can be seen from Table I that the number of unsaturated bonds has no effect on the rotational dynamics of the CSL molecule. This behaviour is found at every temperature within the range studied and confirms our previous results for planar lipid configurations [11]. Apparently, the rotational mobility of CSL molecules in SUVs or liposomes is affected by the temperature only. These results clearly show that a clear distinction must be drawn between molecular orientational order and reorientational dynamics [35–37] and that these two concepts are not necessarily correlated as is widely believed.

Turning to the effects of hydration, the rotational mobility of the CSL molecules is two to three times higher in fully hydrated macroscopically unoriented systems than in planar lipid multibilayers with 24 wt.% of water. Just as was the case for the order parameters, the mobility of CSL in the liposomes and SUVs agrees with the value obtained form extrapolation of the mobility in planar multibilayers [11] to a hydration rate of 35 wt.%. This indicates yet again that the increase in the rotational diffusion of the molecules can be wholly ascribed to the effect of the hydration of the lipid headgroups.

A direct comparison between the diffusion constants reported here and the rotational correlation times, τ, reported in the literature is hampered by the fact that these quantities are not generally related in a transparent way [7,38]. A conversion from diffusion constants to correlation times can only be carried out through the solution of the anisotropy diffusion equation which takes into account the orienting potential, Eqn. 1, experienced by the spin-label molecules. On doing this we obtain for $D_\perp \approx 1.0 \cdot 10^8$ [rad$^2 \cdot$ s^{-1}] rotational correlation times of about 2–3 ns, depending on the potential used. These values can be most readily compared with those reported recently by Kusumi and Pasenkiewicz-Gierula [39] for CSL molecules in liposomes of similar lipids. These authors quote correlation times of about 0.3–0.6 ns obtained from the expression for the lineshapes derived by Israelachvili et al. [40] in the motional-narrowing regime. The question thus arises as to the origin of this large discrepancy in the correlation times.

It is now important to note that in the motional-narrowing analysis the linewidths Γ are given as the sum of two contributions [39,40]:

$$\Gamma = \Gamma_R + \tau \cdot G \qquad (8)$$

where G does not depend on the correlation time τ but is determined by the local orientational distribution of the spin-labels only (Eqn. 4). Γ_R is the residual linewidth arising from effects other than the motion of the molecules. We find that on using these expressions with our values of the correlation times and order parameters, no satisfactory fits of our experimental spectra could be obtained. The main discrepancies arise from the intensity of the central line and the shape of the high-field line.

The fit of the central- and high-field lines can only be improved on reducing the correlation times by a factor of five with a concomitant increase in the residual linewidth Γ_R by nearly a factor of three. The correlation times are now in excellent agreement with those reported by Kusumi and Pasenkiewicz-Gierula [39]. However, the linewidths are dominated by the residual term Γ_R and the motional term $\tau \cdot G$ makes only a small contribution to the spectrum. Therefore the predicted linewidths are insensitive to the details of the orientation distribution, provided $\langle P_2 \rangle$ is kept constant to account for the observed linepositions. As a consequence, widely different models for the molecular order yield satisfactory fits to the observed spectra with the same values for the correlation times τ. The simulations show that the discrepancies between simulations with the SLE and the motional-narrowing formalism can be understood by considering the dynamical contribution to the spectral widths: while with the former method dynamical processes account for almost the total linewidth, the latter analysis requires an independent but dominant contribution Γ_R from residual effects. We believe that these observations invalidate the application of motional-narrowing analysis to our lipid systems. This parallels analogous observations by Freed and co-workers [26] for liquid crystal systems. We note further that the application of the motional-narrowing approximation leads to seriously underestimated values of the rotational correlation times. Unfortunately, such correlation times appear to justify this approach a posteriori.

Comparison with time-resolved fluorescence anisotropy measurements

It will now be instructive to compare the results from ESR experiments on SUVs with those from time-resolved fluorescence anisotropy on the same systems. The probe molecules 1-[4-(trimethylammonio)-phenyl]-6-phenyl-1,3,5-hexatriene (TMA-DPH) used in the latter studies [13] are comparable to the CSL molecules in that they are believed to be anchored at the lipid/water interface [41]. This is also facilitated by the fact that the molecular orientational order and reorientational dynamics of the probe molecules are treated identically in both studies. While the order parameters and diffusion constants are directly comparable, it should be noted that the fluorescence experiments do not monitor the rotation of the TMA-DPH molecules around their long axes. It can be seen from Table II that a reasonable agreement is found for the values of the order parameters $\langle P_2 \rangle$. The value of $\langle P_4 \rangle$, however, is much higher for TMA-DPH than for CSL. The former molecules were found to possess a bimodal orientation distribution function, Eqn. 4, with maxima at $\beta = 0°$ and $\beta = 90°$ (Refs. 13 and 42, and Fig. 4). This was taken to indicate that a fraction of the TMA-DPH molecules lies

TABLE II

Comparison of results from ESR and time-resolved fluorescence anisotropy experiments on SUV suspensions

The probe molecule used in the ESR experiments was CSL. The data for the time-resolved fluorescence anisotropy experiments were taken from Ref. 13. In this work, TMA-DPH was used as a probe molecule.

Lipid	Probe	T(°C)	λ_2	λ_4	$D_\perp$ (10^8 rad$^2 \cdot$s^{-1})	$\langle P_2 \rangle$	$\langle P_4 \rangle$
POPC	CSL	22±1	2.00	0.80	0.40	0.54	0.28
	TMA-DPH	20±2	1.23	2.26	0.90	0.54	0.44
DOPC	CSL	22±1	1.86	0.74	0.50	0.50	0.25
	TMA-DPH	20±2	0.58	2.91	1.6	0.42	0.45
DLPC	CSL	23±1	1.55	0.62	0.50	0.41	0.19
	TMA-DPH	20±2	0.34	3.32	2.7	0.39	0.47

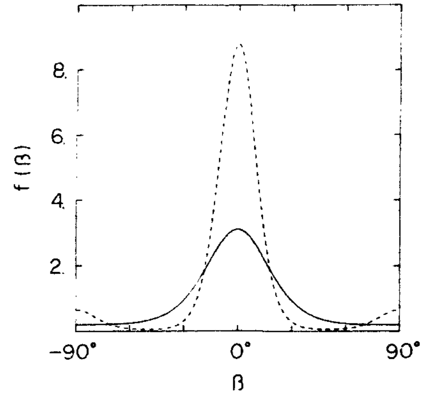

Fig. 4. Distribution function $f(\beta)$ of CSL and TMA-DPH probe molecules relative to the bilayer normal in SUVs of DLPC. (———) CSL; $\lambda_2 = 1.55$, $\lambda_4 = 0.62$. (— — —) TMA-DPH; $\lambda_2 = 0.34$, $\lambda_4 = 3.32$. The corresponding values of $\langle P_2 \rangle$ and $\langle P_4 \rangle$ are given in Table II. Normalization: $\int_\beta f(\beta) \sin \beta \, d\beta = 1$.

at the lipid/water interface of the SUV, parallel to the bilayer surface [13,42]. This can be rationalized on the basis of the observations that the TMA-DPH molecules can partition between the membrane and the water phase [43,44]. For the CSL molecules on the other hand, we have imposed a broad unimodal distribution as they are not expected to exhibit such a partition [45] (Fig. 4).

The different dynamic behaviour exhibited by the two probe molecules in the SUVs is clearly illustrated by the significantly higher values of the diffusion constant $D_\perp$ for TMA-DPH molecules. Furthermore, these rotational rates are quite sensitive to the unsaturation of the fatty acid chains in marked contrasts to the findings with CSL. Interestingly, both probe molecules exhibit similar order parameters and diffusion constants in planar multibilayers [11].

It thus appears that CSL molecules are more reliable probes for monitoring the behaviour of lipids arranged in SUVs.

Conclusions

In this paper we have extended previous experimental work on planar lipid multibilayers to SUV and liposome configurations. The observed differences between these configurations can be ascribed to the state of hydration of the lipid headgroups and the curvature of the bilayer surface.

For every species of lipid molecules studied and any given temperature we find that the order parameter $\langle P_2 \rangle$ decreases in the sequence: planar bilayers > liposomes > SUVs. In contrast, the sequence for the rotational diffusion constants is found to be SUVs ≈ liposomes > planar bilayers. As the lipid headgroups in both the SUV and liposome configurations are fully hydrated, we conclude that the high curvature of the bilayer surface is responsible for the reduction in $\langle P_2 \rangle$, but does not affect the rotational mobility. This moreover confirms our earlier finding that changes in the order and dynamics in lipid bilayer systems are not necessarily correlated.

A comparison of the liposome and planar multibilayer configurations shows that $\langle P_2 \rangle$ and diffusion constants of the CSL molecules agree remarkably well at the same hydration state. Our findings thus indicate that the results obtained from the various configurations form a consistent framework, provided the differences in the hydration of the lipid headgroups and bilayer curvature are taken into account. It should be stressed, however, that macroscopically oriented bilayers provide considerably higher resolution and sensitivity than the orientationally averaged SUV and liposome configurations.

In all the lipid configurations we find that $\langle P_2 \rangle$ decreases on increasing the number of unsaturated bonds of the fatty acid chains. In marked contrast, increasing unsaturation has no noticeable effect on the rotational mobility of the CSL probe molecules. The absence of correlation again shows that the molecular orientational order and reorientational dynamics have to be considered separately.

Compared with the SLE, motional-narrowing analysis seriously underestimates the rotational correlation times. This is noteworthy since such underestimated correlation times seemingly justify the motional-narrowing approach a posteriori. The SLE formalism thus provides the only reliable approach for the interpretation of ESR spectra from lipid systems at physiological temperatures.

Finally, we note that CSL molecules were shown to be more reliable probes for monitoring the order and dynamics in SUVs than the TMA-DPH molecules used in time-resolved fluorescence anisotropy experiments.

Appendix 1

The superposition of spectra from randomly oriented planar bilayers involves a numerical integration over strongly peaked functions. In this situation numerical calculations utilizing a subtraction method will greatly enhance the computational speed and accuracy. The angle-dependent ESR absorption spectra for the planar bilayers are calculated by a numerical solution of the SLE. This results in a separate set of complex eigenvalues and corresponding weight factors for every orientation of the bilayer normal. The ESR absorption spectrum for a given orientation is given by the imaginary part of the complex response function $Z(\omega, \theta)$:

$$P(\omega, \theta) = \operatorname{Im} Z(\omega, \theta) \tag{A-1}$$

$$Z(\omega, \theta) = \sum_i |C_i|^2 / (\omega - \lambda_i) \tag{A-2}$$

where the poles are given by the eigenvalues $\{\lambda_i(\theta)\}$, and $\{C_i(\theta)\}$ are the corresponding weights. Typically, 50 eigenvalues are calculated. Experimentally, the first derivative spectrum $P'(\omega)$ is observed and this is given by

$$d/d\omega P(\omega, \theta) = P'(\omega, \theta) = \mathrm{Im}\, Z'(\omega, \theta) = \mathrm{Im} \sum_i |C_i|^2/(\omega - \lambda_i)^2 \tag{A-3}$$

It is important to note that as a result of the distribution of the eigenvalues, the angle dependent ESR spectra will in general consist of numerous Lorentzian lines. However, the overall lineshape of CSL in the liquid-crystalline phase usually consists of only three distinguishable absorption lines.

SUV and liposome spectra are calculated by the superposition of randomly distributed planar bilayer spectra:

$$P'(\omega) = \mathrm{Im}\, Z'(\omega) \tag{A-4}$$

$$Z'(\omega) = 1/2 \int_{-1}^{1} Z'(\omega, \theta)\, \mathrm{d}\cos\theta \tag{A-5}$$

In our numerical simulation we evaluated $Z'(\omega, \theta)$ at four orientations only, for $\theta = 0°, 45°, 60°$ and $90°$. Each of these simulated lineshapes $Z'(\omega, \theta)$ is fitted to a simple triplet first derivative Lorentzian spectrum $F'(\omega, \theta)$:

$$F'(\omega, \theta) = \sum_{j=1}^{3} R_j(\cos\theta)/[\omega - \Lambda_j(\cos\theta)]^2 \tag{A-6}$$

where R_j and Λ_j are complex numbers. The integration over $\cos\theta$ can be carried out quickly on observing that, while the function $F'(\omega, \theta)$ is strongly peaked, its residues R_j and poles Λ_j are smooth functions of $\cos\theta$, and can be interpolated as:

$$p_0 + p_2 x^2 + p_4 x^4 + p_6 x^6; \quad x = \cos\theta \tag{A-7}$$

The lineshape function $F'(\omega, \theta)$ can now be generated quickly at a sufficiently large number of angles. For our applications the generation of 30 Gaussian points proved adequate for numerical convergence. The background $B'(\omega, \theta) = Z'(\omega, \theta) - F'(\omega, \theta)$ is integrated with a four point integration. The calculated SUV or liposome spectrum is thus given by:

$$P'(\omega) = \mathrm{Im}\, Z'(\omega) = \mathrm{Im}[F'(\omega) + B'(\omega)] \tag{A-8}$$

with

$$F'(\omega) = 1/2 \int_{-1}^{1} F'(\omega, \theta)\, \mathrm{d}\cos\theta$$

and

$$B'(\omega) = 1/2 \int_{-1}^{1} B'(\omega, \theta)\, \mathrm{d}\cos\theta$$

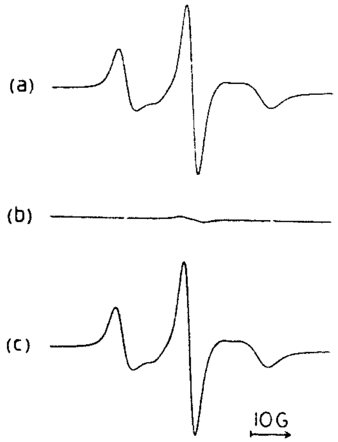

Fig. 5. Example of the simulation of an ESR spectrum for SUV or liposome suspensions. (a) Approximated Lorentzian spectrum Im $F'(\omega)$. (b) Difference spectrum Im $B'(\omega)$. (c) Calculated SUV or liposome spectrum Im $Z'(\omega)$ = Im $F'(\omega)$ + Im $B'(\omega)$. All spectra are broadened with a Gaussian broadening of 1.2 G.

With this subtraction method simulation times are about 10-times faster than with a conventional Gaussian integration of angle dependent spectra. The only caveat in the procedure is that the background signal $B'(\omega)$ can either be accurately evaluated with only four integration points, or makes a negligible contribution to the total lineshape $P(\omega)$. The latter criterium was satisfied in our spectral simulations. A typical simulation is shown in Fig. 5. The procedure can be easily extended in an obvious way to the simulation of spectra consisting of a higher multiplet.

References

1 Schreier-Muccillo, S., Marsh, D., Dugas, H., Schneider, H. and Smith, I.C.P. (1973) Chem. Phys. Lipids 10, 11–27.
2 Stockton, G.W., Polnaszek, C.F., Tulloch, A.P., Hasan, F. and Smith, I.C.P. (1976) Biochemistry 15, 954–966.
3 Kinosita, K., Jr. and Ikegami, A. (1984) Biochim. Biophys. Acta 769, 523–527.
4 Schreier, S., Polnaszek, C.F. and Smith, I.C.P. (1978) Biochim. Biophys. Acta 515, 375–436.
5 Taylor, M.G. and Smith, I.C.P. (1983) Biochim. Biophys. Acta 733, 256–263.
6 Cannon, B., Polnaszek, C.F., Butler, K.W., Eriksson, L.E.G. and Smith, I.C.P. (1975) Arch. Biochem. Biophys. 167, 505–518.
7 Freed, J.H. (1976) in Spin Labeling, Theory and Applications (Berliner, L.J., ed.), pp. 53–132, Academic Press, New York.
8 Lange, A., Marsh, D., Wassmer, K.-H., Meier, P. and Kothe, G. (1985) Biochemistry 24, 4383–4392.
9 Dammers, A.J. (1985) Ph.D. Thesis, Rijksuniversiteit Utrecht, Utrecht.
10 Moser, M., Marsh, D., Meier, P., Wassmer, K.-H. and Kothe, G. (1989) Biophys. J. 55, 111–123.
11 Korstanje, L.J., Van Faassen, E.E. and Levine, Y.K. (1989) Biochim. Biophys. Acta 980, 225–233.
12 Van Langen, H., Engelen, D., Van Ginkel, G. and Levine, Y.K. (1987) Chem. Phys. Lett. 138, 99–104.

13 Van Langen, H., Van Ginkel, G., Shaw, D. and Levine, Y.K. (1989) Eur. Biophys. J. 17, 37–48.

14 Sachse, J.-H., King, M.D. and Marsh, D. (1987) J. Magn. Reson. 71, 385–404.

15 Freed, J.H., Bruno, G.V. and Polnaszek, C.F. (1971) J. Phys. Chem. 75, 3385–3399.

16 Moro, G. and Freed, J.H. (1981) J. Chem. Phys. 74, 3757–3773.

17 Dammers, A.J., Levine, Y.K. and Tjon, J.A. (1988) J. Chem. Phys. 89, 4505–4513.

18 Favro, L.D. (1965) in Fluctuation Phenomena in Solids (Burgess, R.E., ed.), pp. 79–101, Academic Press, New York and London.

19 Nordio, P.L. and Busolin, P. (1971) J. Chem. Phys. 55, 5485–5490.

20 Meirovitch, E. and Freed, J.H. (1984) J. Phys. Chem. 88, 4995–5004.

21 Marriott, T.B., Birrell, G.B. and Griffith, O.H. (1975) J. Am. Chem. Soc. 97, 627–630.

22 Libertini, L.J., Waggoner, A.S., Jost, P.C. and Griffith, O.H. (1969) Proc. Natl. Acad. Sci. USA 64, 13–19.

23 Taylor, M.G. and Smith, I.C.P. (1981) Biochemistry 20, 5252–5255.

24 Morrot, G., Bureau, J.-F., Roux, M., Maurin, L., Favre, E. and Devaux, P.F. (1987) Biochim. Biophys. Acta 897, 341–345.

25 Tanaka, H. and Freed, J.H. (1985) J. Phys. Chem. 89, 350–360.

26 Rao, K.V.S., Polnaszek, C.F. and Freed, J.H. (1977) J. Phys. Chem. 81, 449–456.

27 Korstanje, L.J., Van Faassen, E.E. and Levine, Y.K. (1989) in Reactive and Flexible Molecules in Liquids (Dorfmüller, Th., ed.), in press, Kluwer Academic Publishers, Amsterdam.

28 Madden, K., Kevan, L., Morse II, P.D. and Schwartz, R.N. (1982) J. Am. Chem. Soc. 104, 10–13.

29 Stubbs, C.D., Kouyama, T., Kinosita, K., Jr. and Ikegami, A. (1981) Biochemistry 20, 4257–4262.

30 Kintanar, A., Kunwar, A.C. and Oldfield, E. (1986) Biochemistry 25, 6517–6524.

31 Tanaka, H. and Freed, J.H. (1984) J. Phys. Chem. 88, 6633–6644.

32 Silver, B.L. (1985) in The Physical Chemistry of Membranes, Solomon Press, New York.

33 Seelig, A. and Seelig, J. (1977) Biochemistry 16, 45–50.

34 Van Ginkel, G., Korstanje, L.J., Van Langen, H. and Levine, Y.K. (1986) Faraday Discuss. Chem. Soc. 81, 49–61.

35 Van Ginkel, G., Van Langen, H. and Levine, Y.K. (1989) Biochimie 71, 23–32.

36 Seelig, J. and Seelig, A. (1980) Q. Rev. Biophys. 13, 19–61.

37 Deinum, G., Van Langen, H., Van Ginkel, G. and Levine, Y.K. (1988) Biochemistry 27, 852–860.

38 Nordio, P.L. and Segre, U. (1979) in The Molecular Physics of Liquid Crystals (Luckhurst, G.R. and Gray, G.W., eds.), pp. 411–426, Academic Press, London.

39 Kusumi, A. and Pasenkiewicz-Gierula, M. (1988) Biochemistry 27, 4407–4415.

40 Israelachvili, J., Sjösten, J., Eriksson, L.E.G., Ehrström, M., Gräslund, A. and Ehrenberg, A. (1975) Biochim. Biophys. Acta 382, 125–141.

41 Prendergast, F.G., Haugland, R.P. and Callahan, P.J. (1981) Biochemistry 20, 7333–7338.

42 Van Langen, H., Van Ginkel, G. and Levine, Y.K. (1988) Liq. Cryst. 3, 1301–1317.

43 Kuhry, J.-G., Duportail, G., Bronner, C. and Laustriat, G. (1985) Biochim. Biophys. Acta 845, 60–67.

44 Bronner, C., Landry, Y., Fonteneau, P. and Kuhry, J.-G. (1986) Biochemistry 25, 2149–2154.

45 Hubbell, W.L. and McConnel, H.M. (1969) Proc. Natl. Acad. Sci. USA 63, 16–22.